Volume 14, Issue 4, 142439 (1-12)

Iranian Journal of Catalysis (IJC)

https://doi.org/10.57647/j.ijc.2024.1404.39

New nanoparticles of $NiFe_2O_4$@SiO_2 based tungstate interphase: a highly efficient and selective catalyst for the oxidation of sulfides to sulfoxides

Mohammad Reza Mohammad Shafiee*, Mahnaz Mirheidari, Arshia Eilbeigi

Department of Chemistry, Najafabad Branch, Islamic Azad University, Najafabad, Iran.

Corresponding author: mohammadreza.mohammadshafiee@gmail.com

Review Paper

Received:
31 January 2024
Revised:
31 August 2024
Accepted:
22 September 2024
Published online:
8 October 2024

Abstract:

The study synthesized the novel recoverable alkyl ammonium tungstate (AAT) immobilized on the $NiFe_2O_4$@SiO_2 solid phase ($NiFe_2O_4$@SiO_2-AAT) for the selective oxidation of sulfide to sulfoxide. The catalyst has been characterized by different methods like XRD, FE-SEM, VSM, EDS, FT-IR, and TGA/DTA. The XRD pattern shows the distinctive peaks related to the cubic phase of $NiFe_2O_4$. The catalyst also shows good magnetic characteristics (Ms = 2.5 emu/g) and thermal stability (up to 280 °C. This protocol displays good activity as the catalyst leads to high yields of sulfoxides ($85-99\%$ yields) and performs the green metrics as the catalyst could be recovered 10 times.

Keywords: Magnetic core-shell; $NiFe_2O_4$@SiO_2; Oxidation of sulfide; Sulfoxide; Tungstate interphase catalyst

1. Introduction

Sulfur-containing compounds exhibit various biological activities and have been utilized for their anti-inflammatory, antioxidant, platelet aggregation inhibiting, and cholesterol-reducing properties. Among these compounds, sulfones and sulfoxides have become increasingly significant. They are commonly used as bulk chemicals in different industries and can serve as intermediates for the synthesis of bioactive compounds. Notable sulfoxide compounds like Omeprazole and Pantoprazole are well-known for their role as proton pump inhibitors in treating stomach acid issues (Scheme 1) [1–8].

The oxidation of sulfur compounds, particularly sulfides, has garnered attention from researchers due to the possibilities it presents. Through oxidation, sulfones and sulfoxides can be produced under controlled conditions such as temperature, time, and oxidant quantity. The conversion of sulfides to sulfoxides is generally more challenging than sulfones, requiring a highly selective procedure to prevent further sulfone oxidation [9]. Various methods and catalysts have been explored for the synthesis of sulfoxides, including silica vanadic acid [10], boric acid [11], Br_2/H_2O_2 [12], Fe_3O_4@BNPs@SiO_2-SO_3H [13], silica bromide [14], glacial acetic acid [15], cobalt-based Schiff complex supported on nano-cellulose [16], poly imidazolium-tagged cobalt (II) Schiff base complex [17], alkyl ammonium tungstate bonded to Fe_3O_4@SiO_2 nanoparticles [18], and SnO_2 nanoparticles [19]. However, some of these reported methods have drawbacks, like the use of hazardous solvents, time-intensive procedures, and non-recoverable catalysts.

The oxidation of sulfides to sulfoxides is an important reaction in organic chemistry, with hydrogen peroxide (H_2O_2) often chosen as the oxidizing agent due to its environmental benefits, low cost, and the fact that it produces only water as a by-product. The H_2O_2 compatibility with green chemistry principles makes it a preferred choice for sustainable

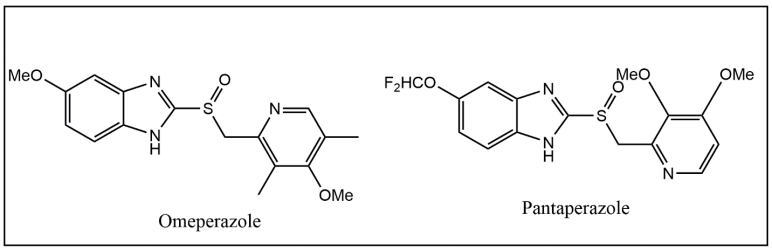

Scheme 1. The structure of omeprazole and pantoprazole as sulfide compounds.

synthesis. While both homogeneous and heterogeneous catalysts have been used to activate H_2O_2, creating efficient, recoverable heterogeneous catalysts remains a significant challenge in this field. Phase transfer catalysts (PTCs) are particularly valuable in oxidation reactions, as they facilitate the interaction of reactants across different phases, enhancing the reaction's efficiency. When PTCs are paired with transition metals, especially in their anionic forms, they enable the use of cost-effective oxidants like H_2O_2. By immobilizing this combination of PTC and transition metal on a solid support, a heterogeneous catalyst is formed, offering the advantages of easier recovery and reuse compared to homogeneous catalysts. This method has shown promise in improving the oxidation of sulfides to sulfoxides, with various transition metals being explored in conjunction with hydrogen peroxide or alkyl peroxides as oxygen sources. This approach not only enhances the efficiency of oxidation but also supports more sustainable chemical processes by minimizing waste and reducing environmental impact. Ongoing research is focused on optimizing these heterogeneous systems to achieve high selectivity and activity, making them more effective and practical for industrial applications [20–29].

To enhance the ability to reuse catalysts, one approach is to modify the catalyst by incorporating magnetic properties. $NiFe_2O_4$, a type of transition metal oxide, is known for its soft ferromagnetic characteristics and has piqued the interest of scientists due to its wide range of applications. Despite its numerous benefits, the synthesis of this material presents challenges such as agglomeration and limited growth potential [30, 31]. One effective way to tackle these challenges is by enveloping the magnetic nanoparticles with biocompatible and non-magnetic substances such as silica. This results in the formation of a core-shell configuration that not only boosts the heat and chemical endurance of the nanoparticles but also amplifies their surface area. The addition of this inactive layer enables additional customization of the material, resulting in enhanced efficiency and reusability of the catalyst [32–36]. Current research demonstrates that metal tungstate (MWO_4) and organic-inorganic hybrids containing WO_4 ions can effectively catalyze oxidation reactions with H_2O_2 as an oxidant. Organic-inorganic hybrids are especially promising due to their high surface area, exceptional catalytic potential, and robust thermal stability, making them highly sought after in catalytic applications. These hybrids have already shown significant efficacy in sulfur oxidation reactions [20–29]. Notably, the catalytic capabilities of $NiFe_2O_4$@SiO_2-based tungstate interphase remain unexplored. Our objective is to develop an innovative $NiFe_2O_4$@SiO_2-based tungstate interphase ($NiFe_2O_4$@SiO_2-AAT), serving as an organic-inorganic hybrid catalyst for the efficient oxidation of sulfides to sulfoxides using H_2O_2. We strongly believe that this new hybrid structure will not only be an ideal catalyst for this oxidation process but also deliver outstanding performance, which is poised to make a significant impact in the field (Scheme 2).

2. Experimental

General

The chemical compounds, including $FeCl_3.6H_2O$, $Si(OEt)_4$, $FeCl_2.4H_2O$, and organic material, were purchased from Merck and Aldrich Companies. The following instruments were used for the catalyst characterization and organic

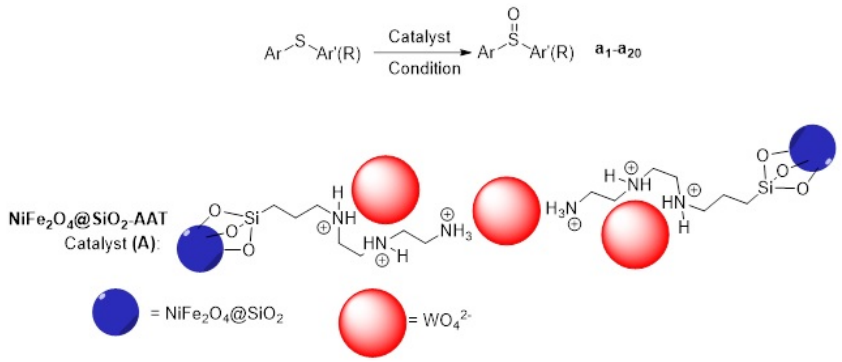

Scheme 2. Oxidation of sulfide to sulfoxides using $NiFe_2O_4$@SiO_2-AAT catalyst.

materials analysis: The X-ray diffraction pattern (XRD) was recorded by X-ray diffractometer (Philips, D5000, Cu-Kα irradiation). The Field emission-scanning electron microscopy (FE-SEM) was obtained by Hitachi S-4160. TGA-DTA analysis was carried out using the TA (Q600) instrument. The FT-IR spectra were recorded as KBr disks using a Thermo (AVATAR) instrument. ^{1}HNMR spectra were recorded on Bruker Avance DPX 400 MHz spectrometer in $CDCl_3$ as solvent relative to TMS (0.00 pm).

Preparation of $NiFe_2O_4$

$NiCl_2.6H_2O$ (20 mmol) and $FeCl_3.6H_2O$ (40 mmol) were dissolved in 100 mL deionized water in a 250 mL beaker under a magnetic stirring. The dilute solution of NH_4OH (20%) was added to the mixture dropwise until the mixture got pH = 10. The obtained solid was washed with deionized water twice and then calcined at 700 °C.

Preparation of $NiFe_2O_4$@SiO_2

$NiFe_2O_4$ nanoparticles (3 g) were dispersed in 150 mL ethanol, and then tetraethyl orthosilicate (7 mL) was added and mixed for 1 h under mechanical stirring. Then, the pH of the solution was adjusted to 8.5 by using NH_4OH (a 20% solution in water) and stirred at room temperature for 48 h. In the end, the magnetic solid ($NiFe_2O_4$@SiO_2) was separated by a magnet, washed thoroughly with water, and dried at 100 °C in the air atmosphere.

Preparation of $NiFe_2O_4$@SiO_2-AAT

To functionalize the solid support, $NiFe_2O_4$@SiO_2 (5 g) and N-(2-aminoethyl)-N′- (3-(trimethoxysilyl)propyl)ethane-1,2-diamine (2.5 mmol) were dispersed in toluene (100 mL) and refluxed for 24 h (Scheme 2, Intermediate A). The obtained solid was separated, washed with toluene, and dried at 70 °C. In the next step, the functionalized $NiFe_2O_4$@SiO_2 (5 g) was dispersed in 100 mL CH_3Cl and then drop by drop mixed with triflic acid and stirred for 10 h (Scheme 3, Intermediate B). Afterward, the solvent of the product was evaporated, and the obtained solid was washed with deionized water and combined with sodium tungstate (10 M, 50 mL). In the end, the resulting solid was separated, washed with ethanol, and dried.

Measuring acidity using the $BaWO_4$ test

The prepared catalyst (1 g) was dispersed in 100 mL of deionized water and mixed with barium chloride (1 M). The sample was placed at room temperature for precipitation of $BaWO_4$. After completion of precipitation, the collected solid was precisely measured and used for estimating the quantity of tungstate. The value of tungstate for the catalyst was 1.14 mmol/g. According to this, the capacity of positive hydrogen ions (H^+) in the sample was measured at 2.28 mmol H^+/g.

General procedure:

$NiFe_2O_4$@SiO_2-AAT (0.025 g) was added to the mixture of sulfide (2 mmol) and H_2O_2 (30%, 6 eq) in 10 mL ethanol and mixed under stirring at room temperature until the completion of the reaction (monitored by TLC). After the reaction progressed, the catalyst was separated by an external magnetic. Then, the solvent under reduced pressure was removed and the products were purified by silica gel column chromatography.

Spectral data

Methyl phenyl sulfoxide (a_1): white solid; ^{1}HNMR (500 MHz, $CDCl_3$): δ = 2.72 (s, 3H, CH_3), 7.44 – 7.53 (m, 3H), 7.19 (d, J = 7.8 Hz, 2H).

Benzyl phenyl sulfoxide (a_3): white solid; m.p.: 127 – 129 °C, ^{1}HNMR (500 MHz, $CDCl_3$): δ = 4.03 (d, J = 12.8 Hz, 1H), 4.16 (d, J = 12.8 Hz, 1H), 6.98 (t, J = 8.0 Hz, 2H), 7.19 (t, J = 8.0 Hz, 1H), 7.27 – 7.50 (m, 7H).

Benzyl p-tolyl sulfoxide (a_4): white solid; m.p.: 139 – 141 °C; ^{1}HNMR (500 MHz, $CDCl_3$): δ = 2.41 (s, 3H), 3.96 (d, J = 12.4 Hz, 1H), 4.07 (t, J = 12.4 Hz, 1H), 6.98 (d, J = 7.8 Hz, 2H), 7.18 – 7.40 (m, 7H).

4-methoxybenzyl p-tolyl sulfoxide (a_5): white solid; m.p.: 123 – 125 °C; ^{1}HNMR (500 MHz, $CDCl_3$): δ = 2.38 (s, 3H), 3.83 (s, 3H), 3.92 (d, J = 12.6 Hz, 1H), 4.01 (t, J = 12.6 Hz, 1H), 6.78 (d, J = 7.8 Hz, 2H), 6.99 (d, J = 7.8 Hz, 2H), 7.19 (d, J = 7.6 Hz, 2H), 7.28 (d, J = 7.6 Hz, 2H).

Benzyl 2-methoxyphenyl sulfoxide (a_6): Oil; ^{1}HNMR (500 MHz, $CDCl_3$): δ = 3.86 (s, 3H), 3.95 (d, J = 12.6 Hz, 1H), 6.92 (d, J = 7.8 Hz, 1H), 6.97 (d, J = 7.8 Hz, 1H), 7.03 (t, J = 7.6 Hz, 1H), 7.11 (t, J = 7.6 Hz, 1H), 7.17 – 7.31 (m, 3H), 7.43 (d, J = 7.6 Hz, 2H).

Benzyl 3-methoxyphenyl sulfoxide (a_7): Oil; ^{1}HNMR (500 MHz, $CDCl_3$): δ = 3.74 (s, 3H), 3.97 (d, J = 12.6 Hz, 1H), 4.11 (d, J = 12.6 Hz, 1H), 6.88 – 7.33 (m, 7H), 7.45 (d, J = 7.6 Hz, 2H).

3. Result and discussion

In Scheme 3, the synthesis of a new immobilized alkyl ammonium tungstate (AAT) sample ($NiFe_2O_4$@SiO_2-AAT) involves several key steps. The process begins with the creation of intermediate **A** by reacting c nanoparticles with N-(2-aminoethyl)-N′-(3-(trimethoxysilyl)propyl)ethane-1,2-diamine. This reaction functionalizes the silica-coated magnetic nanoparticles with amine groups, preparing them for further modifications. Following this, intermediate **B** is generated through the protonation of amine groups using trifluoromethanesulfonic acid (triflic acid), resulting in the formation of ammonium groups. The final catalyst is obtained by replacing the triflate anions with tungstate ions via ion exchange using sodium tungstate. This step is essential for integrating tungsten into the material, which imparts the desired catalytic properties. The synthesized catalyst was characterized using various analytical techniques to determine its structural, morphological, and elemental properties.

X-ray diffraction (XRD) analysis, depicted in Figure 1, was utilized to assess the crystalline structure of both the unmodified $NiFe_2O_4$ and the modified $NiFe_2O_4$@SiO_2-AAT

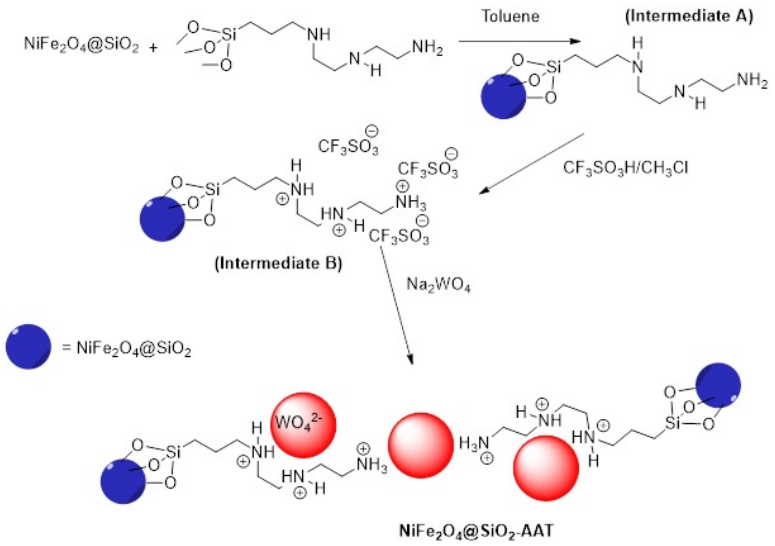

Scheme 3. Preparation of $NiFe_2O_4$@SiO_2-AAT.

samples. The XRD patterns revealed distinct peaks at specific 2θ values, including 12, 18.3, 30.2, 35.7, 37.3, 43.4, 47.3, 53.8, 62.7, 71.4, 74.6, and 79.0 [2θ°]. These peaks indicate the presence of a crystalline phase with high purity and structural order.

The FT-IR spectra provided a detailed analysis of the functional groups present on the surface of the $NiFe_2O_4$@SiO_2-AAT sample (Figure 2). Peaks detected at 3693 and 3668 cm^{-1} were linked to the N-H stretching vibrations, indicating amine groups on the sample surface. The peaks at 2989, 2958, and 1367 cm^{-1} were associated with C-H bonds, pointing to the presence of alkyl groups in the material's structure. Additionally, peaks at 1273 and 1201 cm^{-1} were attributed to C-N bonds, suggesting the integration of nitrogen-containing functional groups. Further, the peaks at 1612, 1043, and 938 cm^{-1} confirmed the presence of Si-O-Si and Si-OH groups, which are indicative of the silica framework and surface hydroxyl groups. The strong peaks observed around 880 and 698 cm^{-1} were linked to the vibrations of O-W-O and W=O bonds, suggesting the presence of tungsten oxides within the structure. Finally, the peak at 532 cm^{-1} was characteristic of the Fe-O and Ni-O bonds, confirming the presence of metal-oxygen bonds typical of the $NiFe_2O_4$ spinel structure. This analysis highlights the complex surface chemistry and the multi-functional composition of the $NiFe_2O_4$@SiO_2-AAT sample.

To investigate the physical characteristics of the catalyst, scanning electron microscopy (SEM) was employed, as shown in Figure 3. The SEM images revealed that the nanoparticles were uniformly distributed, with no significant aggregation, and had an average size of less than 100 nm. This uniformity and small size are advantageous for catalytic activity, as they increase the surface area available for reactions. Energy-dispersive X-ray spectroscopy (EDS), shown in Figure 4, was used to analyze the elemental composition of the catalyst. The EDS results confirmed

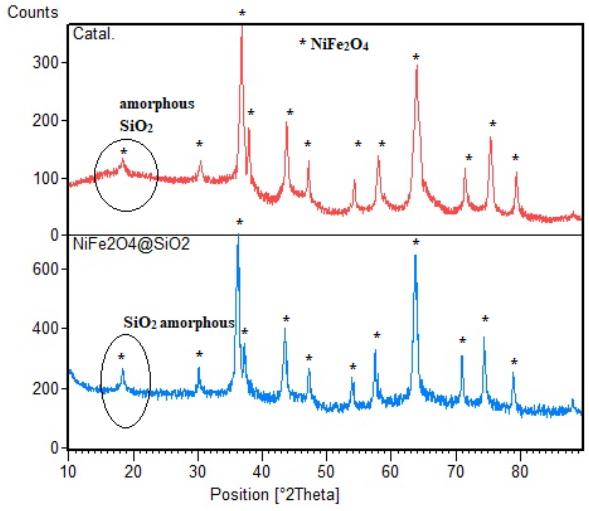

Figure 1. XRD analysis for $NiFe_2O_4$@SiO_2 and $NiFe_2O_4$@SiO_2-AAT samples.

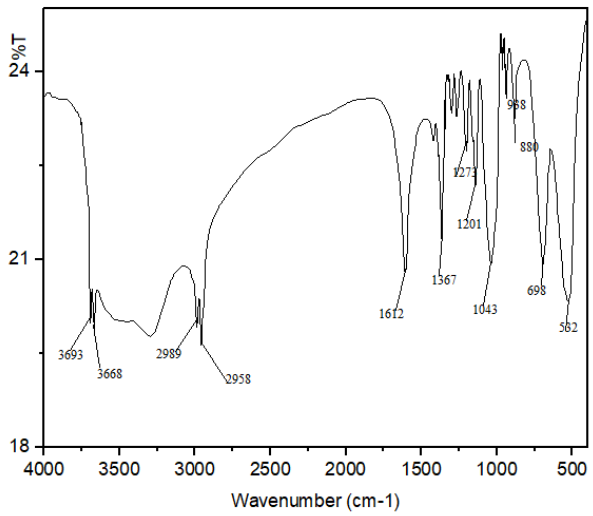

Figure 2. FT-IR analysis of $NiFe_2O_4$@SiO_2-AAT sample.

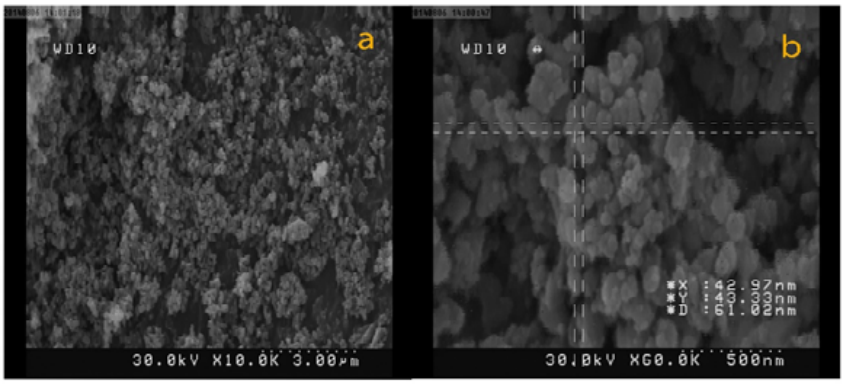

Figure 3. SEM images of $NiFe_2O_4$@SiO_2-AAT sample.

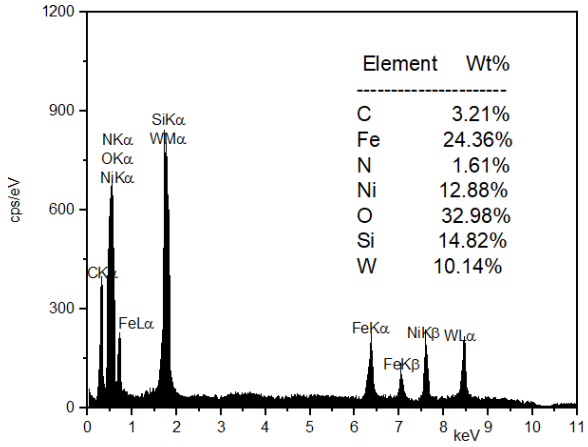

Figure 4. EDS analysis of $NiFe_2O_4$@SiO_2-AAT sample.

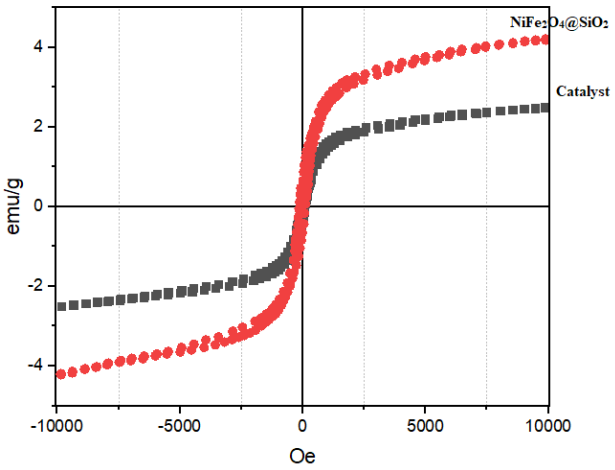

Figure 5. VSM spectra for $NiFe_2O_4$@SiO_2 and NiFe2O4@SiO2-AAT samples.

the presence of iron (Fe), nickel (Ni), silicon (Si), oxygen (O), carbon (C), nitrogen (N), and tungsten (W) within the sample. This comprehensive elemental analysis verified the successful incorporation of all intended elements, demonstrating the effectiveness of the synthesis process and confirming the chemical composition of the final product. Overall, these characterization techniques provided a thorough understanding of the catalyst's structural, morphological, and compositional attributes, which are crucial for evaluating its potential efficacy in various catalytic applications.

The magnetic properties of the catalyst were investigated by VSM analysis. The saturated magnetization for $NiFe_2O_4$@SiO_2 is about 4 emu/g. The saturation magnetization (Ms) for the catalyst is about 2.5 emu/g. The decrease in the value of saturation magnetization is due to functionalization (Figure 5).

Figure 6 shows the TGA and DTA curves for the catalyst. The first weight loss (about 5%) occurs until 280 °C for evaporation of absorbed water. The second weight loss (35%) happens from 290 to 900 °C and belongs to the process of decomposition for organic groups in the catalyst. The high temperature required for decomposition confirms the thermal stability of the catalyst.

After confirmation of the accuracy of the prepared catalyst,

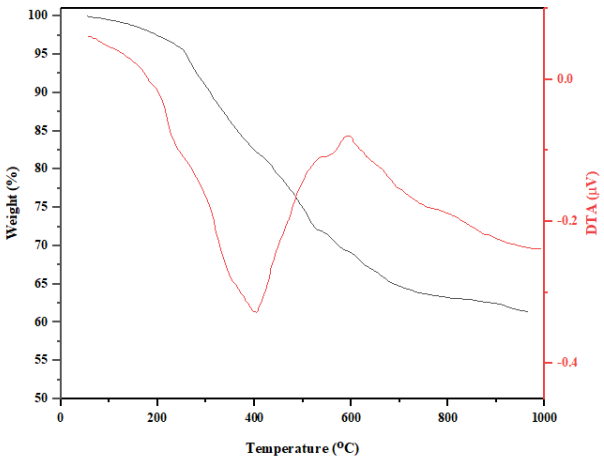

Figure 6. TGA/DTA curves of $NiFe_2O_4$@SiO_2-AAT sample.

the efficiency of the catalyst was studied to prepare sulfoxides by oxidation of organic sulfides in the presence of H_2O_2. To make optimal conditions, different conditions were investigated for the oxidation of methyl phenyl sulfide (2 mmol) as a model reactant. First, different solvents were

Table 1. Optimization of the reaction conditions.

Entry	Catalyst (g)	Condition	Time (h)	Yield (%)
1	0.025	EtOH, r.t.; H_2O_2 (30%, 6eq)	1	98
2	0.025	EtOH, r.t.; H_2O_2 (30%, 4eq)	1	75
3	0.025	EtOH, r.t.; H_2O_2 (30%, 2eq)	1	19
4	0.025	Hexane, r.t.; H_2O_2 (30%, 6eq)	2	-
5	0.025	CH_2Cl_2, r.t.; H_2O_2 (30%, 6eq)	2	-
6	0.025	$CHCl_3$, r.t.; H_2O_2 (30%, 6eq)	1.5	25
7	0.025	Toluene, r.t.; H_2O_2 (30%, 6eq)	1.5	-
8	0.025	DMF, r.t.; H_2O_2 (30%, 6eq)	2	56
9	0.025	H_2O, r.t.; H_2O_2 (30%, 6eq)	3	55
10	0.025	EtOAc, r.t.; H_2O_2 (30%, 6eq)	1.5	28
11	0.01	EtOH, r.t.; H_2O_2 (30%, 6eq)	2	21
12	0.05	EtOH, r.t.; H_2O_2 (30%, 6eq)	1	96
13	0.075	EtOH, r.t.; H_2O_2 (30%, 6eq)	1	93
14	0.1	EtOH, r.t.; H_2O_2 (30%, 6eq)	1	94
15	0.05 (A)	EtOH, r.t.; H_2O_2 (30%, 6eq)	1	37*
16	0.05 (B)	EtOH, r.t.; H_2O_2 (30%, 6eq)	1	64**
17	-	EtOH, r.t.; H_2O_2 (30%, 6eq)	1	-***

*Isolated yield for intermediate A; ** intermediate B; ***without catalyst

tested in the reaction. Results revealed that the oxidation process rate increased in ethanol as a solvent. Then, different amounts of H_2O_2 and catalyst ($NiFe_2O_4$@SiO_2-AAT) were evaluated for the model test. The obtained outcomes showed methyl phenyl sulfide (2 mmol) has better conversion to sulfoxide (98%) in the presence of 0.025 g catalyst and 6 eq H_2O_2 (Table 1). Without catalysts, the reaction is not able to proceed, and in the presence of intermediates A and B (Scheme 3), a low yield of product was formed.

The combination of tungstate (WO_4) and hydrogen peroxide (H_2O_2) is an effective catalytic system for the oxidation of sulfides to sulfoxides. The mechanism generally involves the formation of cyclic peroxotungstate species, which act as the active oxidant in the reaction. According to the reported literature [20–29], the W=O bond is oxidized by H_2O_2 to form a cyclic peroxotungstate complex form, and the sulfides could be oxidized to sulfoxides by this active intermediate of the catalyst (Figure 7).

Under the optimized condition, the scope and limitations of the work were explored for efficient sulfide oxidation. A range of aromatic and non-aromatic sulfoxides were prepared in high yields. The procedure used is clean, inexpensive, and utilizes aqueous hydrogen peroxide as an oxidant. Significantly, the use of aromatic and naphthyl sulfides results in excellent yields in reasonably short reaction times. However, electron-donation groups substituted on the aromatic rings could increase the reaction rate, and halogen atoms such as Br and Cl decreased the rate of the reaction. Interestingly, the yields in all cases are high (Table 2).

After ending the reaction, the catalyst was separated from

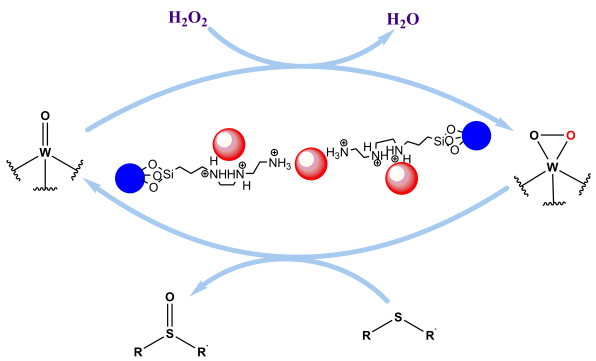

Figure 7. Oxidation of sulfides to sulfoxides using tungstate (WO_4) ions.

Table 2. Preparation of sulfoxide in the presence of $NiFe_2O_4$@SiO_2-AAT[a].

Entry	Sulfide	Product	Time (h)	Yield (%)[b]
1	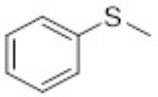	a_1	1	98
2	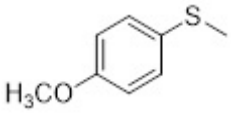	a_2	1	98
3	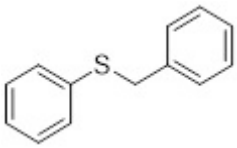	a_3	1	95
4	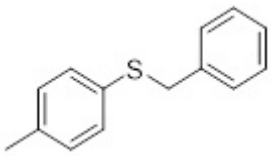	a_4	1	98
5	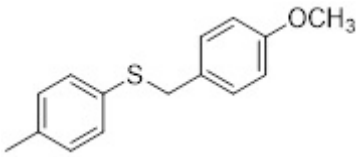	a_5	1	99
6	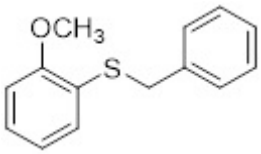	a_6	1.5	97
7	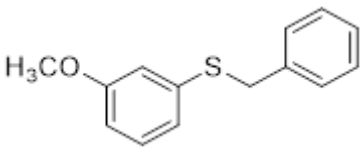	a_7	1	98
8	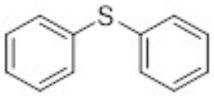	a_8	1.5	96
9	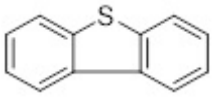	a_9	2	95

Continue of Table 2.

Entry	Sulfide	Product	Time (h)	Yield (%)[b]
10	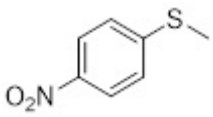	a_{10}	2	93
11	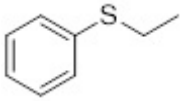	a_{11}	1.5	91
12		a_{12}	1.5	88
13	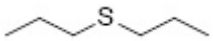	a_{13}	1.5	85
14	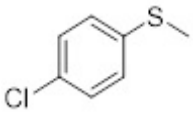	a_{14}	2	99
15	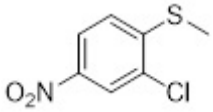	a_{15}	2.5	89
16	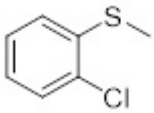	a_{16}	1	96
17	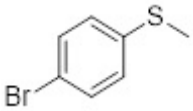	a_{17}	2	92
18	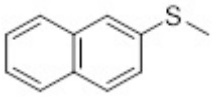	a_{18}	1.5	96
19		a_{19}	1.5	91
20	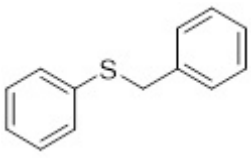	a_{20}	1.5	97

[a] Reaction conditions: sulfide (2 mmol), 30 % H_2O_2 (6eq), $NiFe_2O_4$@SiO_2-AAT (0.025 g), Ethanol (10 ml) at room temperatures
[b] Isolated yields

Table 3. TON and TOF calculations.

Sulfide	Product	TON	TOF (s^{-1})
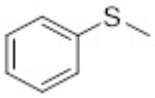	a_1	17.19	0.0047
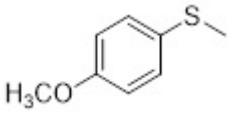	a_2	17.19	0.0047
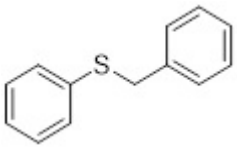	a_3	16.67	0.0046

Table 4. Comparison results of the oxidation of methyl phenyl sulfide.

Catalyst	Condition	Time / Yield (%)	Ref.
$NiFe_2O_4$@SiO_2-AAT	EtOH, r.t.; H_2O_2 (30%, 3mmol)	1h / 98	This work
Silica-based tungstate interphase	H_2O_2 (30%, 3-8eq), CH_2Cl_2/CH_3OH	1.5h / 82	[19]
Urea-hydrogen peroxide (2eq)	85°C,	15min / 80	[37]
$Ti(SO_4)_2$/GOF	CH_3OH, r.t.; H_2O_2 (30%, 6.5mmol)	0.5h / 98	[38]
Fe_3O_4@SiO_2-APTES($Fe(acac)_2$)	CH_3CN, r.t.; H_2O_2 (30%, 1.5mmol)	6h / 74	[39]
Zr/SiW_{12}/GO	Solvent-free, r.t.; H_2O_2 (30%, 2eq)	20min / 95	[40]
$MgWO_4$	EtOH, r.t.; H_2O_2 (30%, 3mmol)	2h / 23	This work
Na_2WO_4	EtOH, r.t.; H_2O_2 (30%, 3mmol)	2h / trace	This work
$CaWO_4$	EtOH, r.t.; H_2O_2 (30%, 3mmol)	2h / 18	This work
$ZnWO_4$	EtOH, r.t.; H_2O_2 (30%, 3mmol)	2h / 22	This work

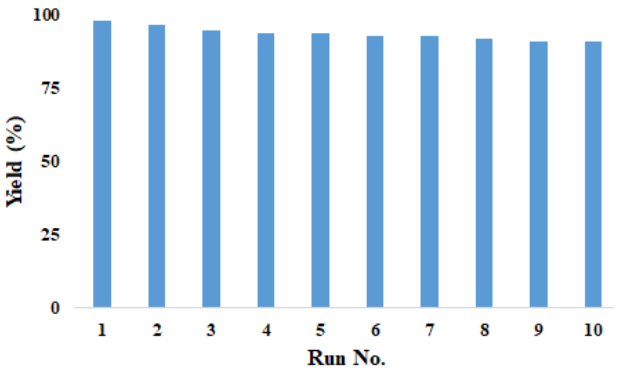

Figure 8. Recycling results for $NiFe_2O_4$@SiO_2-AAT.

the reaction with an external magnet that was washed completely with ethanol and applied once more to the reaction. The obtained outcome of the reaction displays that the catalyst can be used 10 times with no clear reduction in yield (Figure 8).

This work has the advantages of good turnover number (TON) and turnover frequency (TOF) values. The TON and TOF values were calculated using the following equations:

$$\text{TOF} = \frac{\text{TON}}{\text{Time}}$$

$$\text{TON} = \frac{\text{Number of product mol}}{\text{Number of active site of catalyst (mol)}}$$

The catalyst value is 0.025 g (0.057 mmol H^+), and sulfide is 2 mmol.

Notably, all of the reactions have high yields of desired products and lead to high values of TON and TOF (Table 3).

The catalytic performance of $NiFe_2O_4$@SiO_2-AAT, as shown in Table 4, clearly surpasses other Lewis and Brønsted acid catalysts, particularly when considering reaction time and yield. Under the same reaction conditions, $NiFe_2O_4$@SiO_2-AAT exhibits superior activity compared to catalysts like $MgWO_4$, Na_2WO_4, $CaWO_4$, and $ZnWO_4$. Additionally, its catalytic effectiveness is on par with several well-established catalysts from the literature, such as silica-based tungstate interphase, urea-hydrogen peroxide, $Ti(SO_4)_2$/GOF, Fe_3O_4@SiO_2-APTES($Fe(acac)_2$), and Zr/SiW_{12}/GO. These findings highlight the exceptional potential of $NiFe_2O_4$@SiO_2-AAT as a catalyst for various chemical processes.

4. Conclusion

In conclusion, this research established that $NiFe_2O_4$@SiO_2-AAT can be efficiently synthesized through a straightforward process, resulting in a highly effective and eco-friendly nano-catalyst for converting sulfides to sulfoxides using 30% H_2O_2 at room temperature. The catalyst offers several practical benefits, including easy magnetic separation, which simplifies recovery and reduces the need for additional purification steps. It consistently delivers high sulfoxide yields while also shortening reaction times, making the process more efficient. One of the most significant advantages of this catalyst is its durability and reusability. It can be recycled through simple filtration and reused in up to 10 cycles without noticeable degradation in performance, highlighting its potential for sustainable, long-term use. These characteristics make $NiFe_2O_4$@SiO_2-AAT a strong candidate for large-scale industrial applications, particularly where cost efficiency, ease of operation, and environmental considerations are critical. This work points to its promise as a versatile material for advancing green chemistry in practical settings.

Acknowledgments

We are thankful to the Najafabad Branch, Islamic Azad University Research Council, for partial support of this research.

Authors contributions

M.R. Mohammad Shafiee is the corresponding author of the work and performs financial support and data analysis. M. Mirheidari and A. Eilbeigi performed the experiments and wrote the paper. All authors have read and agreed to the published version of the manuscript.

Availability of data and materials

There is no data available associated with this manuscript.

Conflict of interests

The authors declare that they have no conflict of interest to be declared.

References

[1] D.Y. Lee, H. Li, H.J. Lim, H.J. Lee, R. Jeon, and J.-H. Ryu. *J. Med. Food*, **15**(2012):992–999. DOI: https://doi.org/10.1089/jmf.2012.2275.

[2] H. Lim, K. Kubota, A. Kobayashi, T. Seki, and

T. Ariga. *Biosci. Biotech. Biochem.*, **63**(1999):298–301. DOI: https://doi.org/10.1271/bbb.63.298.

[3] E. Mukwevho, Z. Ferreira, and A. Ayeleso. *Molecules*, **19**(2014):19376–19389. DOI: https://doi.org/10.3390/molecules191219376.

[4] M.S. Subramanian, M.S.G. Nandagopal, S. Amin Nordin, K. Thilakavathy, and N. Joseph. *Molecules*, **25**(2020):4111. DOI: https://doi.org/10.3390/molecules25184111.

[5] I. Fernandez and N. Khiar. *Chem. Rev.*, **103**(2003): 3651–3706. DOI: https://doi.org/10.1021/cr990372u.

[6] K. Khosravi, S. Naserifar, and A. Asgari. *Lett. Org. Chem.*, **13**(2016):749–756. DOI: https://doi.org/10.2174/1570178614666161123115100.

[7] A. Padwa, W.H. Bullock, and A.D. Dyszlewski. *J. Org. Chem.*, **55**(1990):955–964. DOI: https://doi.org/10.1021/jo00290a029.

[8] R.V. Kupwade. *J. Chem. Rev.*, **1**(2019):99–113. DOI: https://doi.org/10.33945/SAMI/JCR.2019.1.99113.

[9] A. Taketoshi, P. Concepción, H. Garcia, A. Corma, and M. Haruta. *Bull. Chem. Soc. Jap.*, **86**(2013):1412–1418. DOI: https://doi.org/10.1246/bcsj.20130075.

[10] M.A. Zolfigol, A. Khazaei, M. Safaiee, M. Mokhlesi, R. Rostamian, M. Bagheri, M. Shiri, and H.G. Kruger. *J. Mole. Catal. A Chem.*, **370**(2013):80–86. DOI: https://doi.org/10.1016/j.molcata.2012.12.015.

[11] A. Rostami and J. Akradi. *Tetrahedron Lett.*, **51**(2010):3501–3503. DOI: https://doi.org/10.1016/j.tetlet.2010.04.103.

[12] A. Bravo, B. Dordi, F. Fontana, and F. Minisci. *J. Org. Chem.*, **66**(2001):3232–3234. DOI: https://doi.org/10.1021/jo0017178.

[13] M.G. Kermanshahi and K. Bahrami. *RSC Adv.*, **9**(2019):36103–36112. DOI: https://doi.org/10.1039/C9RA06221A.

[14] B. Maleki, S. Hemmati, A. Sedrpoushan, S.S. Ashrafi, and H. Veisi. *RSC Adv*, **4**(2014):40505–40510. DOI: https://doi.org/10.1039/C4RA06132B.

[15] H. Golchoubian and F. Hosseinpoor. *Molecules*, **12**(2007):304–311. DOI: https://doi.org/10.3390/12030304.

[16] M.-S. Mashhoori, R. Sandaroos, and A. Zeraatkar Moghaddam. *Polycycl. Arom. Compd.*, **42**(2022):5067–5085. DOI: https://doi.org/10.1080/10406638.2021.1922470.

[17] R. Sandaroos, B. Maleki, S. Naderi, and S. Peiman. *Inorg. Chem. Commun.*, **148**(2023):110294. DOI: https://doi.org/10.1016/j.inoche.2022.110294.

[18] S.M. Khatami, M. Khalaj, and M. Ghashang. *Iran. J. Catal.*, **13**(2023):475–485. DOI: https://doi.org/10.30495/ijc.2023.1993331.2039.

[19] M. Dehbashi, M. Aliahmad, M.R.M. Shafiee, and M. Ghashang. *Phosphorus, Sulfur Relat. Elem.*, **188**(2013):864–872. DOI: https://doi.org/10.1080/10426507.2012.717139.

[20] B. Karimi, M. Ghoreishi-Nezhad, and J.H. Clark. *Org. Lett.*, **7**(2005):625–628. DOI: https://doi.org/10.1021/ol047635d.

[21] C. Rajkumar, B. Thirumalraj, S.-M. Chen, P. Veerakumar, and S.-B. Liu. *ACS Appl. Mater. Interfaces*, **9**(2017):31794–31805. DOI: https://doi.org/10.1021/acsami.7b07645.

[22] B. Karimi and M. Khorasani. *ACS Catal*, **3**(2013): 1657–1664. DOI: https://doi.org/10.1021/cs4003029.

[23] M. Dabiri, H. Esmaielie Tavil, N. Farajinia Lehi, S. Kazemi Movahed, A. Mnachekanian Salmasi, and S. Souri. *J. Phys. Chem. Solids*, **162**(2022):110497. DOI: https://doi.org/10.1016/j.jpcs.2021.110497.

[24] F. Rajabi, E. Vessally, R. Luque, and L. Voskressensky. *Mol. Catal*, **515**(2021):111931. DOI: https://doi.org/10.1016/j.mcat.2021.111931.

[25] M. Jin, J. Wang, B. Wang, Z. Guo, and Z. Lv. *Micropor. Mesopor. Mat.*, **277**(2019):84–94. DOI: https://doi.org/10.1016/j.micromeso.2018.10.021.

[26] A. Sedrpoushan, F. Hosseini-Eshbala, F. Mohanazadeh, and M. Heydari. *Appl. Organomet. Chem.*, **32**(2018):e4004. DOI: https://doi.org/10.1002/aoc.4004.

[27] S.H. Hosseini, M. Tavakolizadeh, N. Zohreh, and R. Soleyman. *Organomet. Chem.*, **32**(2018):e3953. DOI: https://doi.org/10.1002/aoc.3953.

[28] N. Zohreh, S.H. Hosseini, A. Pourjavadi, R. Soleyman, and C. Bennett. *J. Indust. Eng. Chem.*, **44**(2016):73–81. DOI: https://doi.org/10.1016/j.jiec.2016.08.011.

[29] C.M. Tressler, P. Stonehouse, and K.S. Kyler. *Green Chem.*, **18**(2016):4875–4878. DOI: https://doi.org/10.1039/C6GC00725B.

[30] S. Iraqui, S.S. Kashyap, and M.H. Rashid. *Nanoscal. Adv.*, **2**(2020):5790–5802. DOI: https://doi.org/10.1039/D0NA00591F.

[31] L. Sun, R. Zhang, Z. Wang, L. Ju, E. Cao, and Y. Zhang. *J. Mag. Mag. Mater.*, **421**(2017):65–70. DOI: https://doi.org/10.1016/j.jmmm.2016.08.003.

[32] R. Hajiarab, M.R. Mohammad Shafiee, and M. Ghashang. *Polycycl. Aromat. Compd.*, **43**(2023):2032–2043, . DOI: https://doi.org/10.1080/10406638.2022.2039231.

[33] R. Hajiarab, M.R. Mohammad Shafiee, and M. Ghashang. *Org. Prep. Proced. Int.*, **54**(2022):259–267, . DOI: https://doi.org/10.1080/00304948.2022.2033064.

[34] F. Aminsharei, A. Lahijanian, A. Shiehbeigi, S.S. Beiki, and M. Ghashang. *Int. J. Biolog. Macromol.*, **276**(2024):134004. DOI: https://doi.org/10.1016/j.ijbiomac.2024.134004.

[35] F. Rezaei, H. Alinezhad, and B. Maleki. *Sci Rep*, **13**(2023):20562. DOI: https://doi.org/10.1038/s41598-023-47794-2.

[36] H. Boroumand, H. Alinezhad, B. Maleki, and S. Peiman. *Polycyclic Aromatic Compounds*, **43**(2023):7853–7869. DOI: https://doi.org/10.1080/10406638.2022.2140683.

[37] R.S. Varma and K.P. Naicker. *Org. Lett.*, **1**(1999): 189–191. DOI: https://doi.org/10.1021/ol990522n.

[38] Q. Wang, W. Ma, Q. Tong, G. Du, J. Wang, M. Zhang, H. Jiang, H. Yang, Y. Liu, and M. Cheng. *Sci. Rep.*, **7**(2017):7209. DOI: https://doi.org/10.1038/s41598-017-07590-1.

[39] A. Bayat, M. Shakourian-Fard, N. Ehyaei, and M. Mahmoodi Hashemi. *RSC Adv.*, **4**(2014):44274–44281. DOI: https://doi.org/10.1039/C4RA07356H.

[40] Z. Yekke-Ghasemi, M.M. Heravi, M. Malmir, and M. Mirzaei. *Sci. Rep.*, **13**(2023):16752. DOI: https://doi.org/10.1038/s41598-023-43985-z.